Evaluating systematic dependencies of Type Ia supernovae

A. C. Calder,[1,2] B. K. Krueger,[1] A. P. Jackson,[1] D. M. Townsley,[3] F. X. Timmes,[4] E. F. Brown,[5] and D. A. Chamulak[6]

[1]Department of Physics and Astronomy, Stony Brook University, Stony Brook, NY 11794-3800
[2]New York Center for Computational Sciences, Stony Brook University, Stony Brook, NY 11794-3800
[3]Department of Physics and Astronomy The University of Alabama, Tuscaloosa, AL 35487-0324
[4]School of Earth and Space Exploration, Arizona State University, Tempe, AZ 85287-1404
[5]Department of Physics and Astronomy, Michigan State University, East Lansing, MI 48824-2320
[6]Physics Division, Argonne National Laboratory, Argonne, IL 60439

E-mail: acalder@mail.astro.sunysb.edu

Abstract. Type Ia supernovae are bright stellar explosions thought to occur when a thermonuclear runaway consumes roughly a solar mass of degenerate stellar material. These events produce and disseminate iron-peak elements, and properties of their light curves allow for standardization and subsequent use as cosmological distance indicators. The explosion mechanism of these events remains, however, only partially understood. Many models posit the explosion beginning with a deflagration born near the center of a white dwarf that has gained mass from a stellar companion. In order to match observations, models of this single-degenerate scenario typically invoke a subsequent transition of the (subsonic) deflagration to a (supersonic) detonation that rapidly consumes the star. We present an investigation into the systematics of thermonuclear supernovae assuming this paradigm. We utilize a statistical framework for a controlled study of two-dimensional simulations of these events from randomized initial conditions. We investigate the effect of the composition and thermal history of the progenitor on the radioactive yield, and thus brightness, of an event. Our results offer an explanation for some observed trends of mean brightness with properties of the host galaxy.

1. Introduction

Type Ia supernovae (SNe Ia) are bright stellar explosions distinguished principally by a lack of hydrogen and strong silicon features in their spectra (for reviews, see [1,2]). Properties of the light curves of these events allow their use as distance indicators at cosmological distances [3,4,5], and these are at present the most powerful and best proved technique for studying dark energy [6,7,8,9,10]. Accordingly, there are many observational campaigns underway striving to gather information about the systematics of these events and to better measure the expansion history of the Universe (see [11]

and references therein). These events are also responsible for producing many of the heavy (iron-group) elements found in the galaxy and are therefore critical to galactic chemical evolution [12].

Despite their widespread use as distance indicators and their importance to galactic chemical evolution, much of what is known about SNe Ia follows from empirical relationships, not a theoretical understanding of the explosion mechanism. Motivated principally by cosmological studies, observational campaigns are uncovering the rich phenomenology of these events at an unprecedented rate and the future promises even more (the Dark Energy Survey, LSST, JDEM, see [13]). Accordingly, the goal of modeling SNe Ia is a theoretical understanding of the observed properties, particularly the intrinsic scatter of these events and the source of any systematic trends. Understanding and quantifying these are essential to their effective use as distance indicators [5,14].

A widely accepted view is that SNe Ia are the thermonuclear incineration of a white dwarf composed principally of carbon and oxygen that has gained mass from a companion star [2]. In this scenario, the white dwarf gains mass, compressing the core until an explosion ensues. Recent observational evidence, however, does suggest other progenitors such as the merging of two white dwarf may explain many events [15,16,17]. Regardless of the exact mechanism, the "upshot" is that these events synthesize ~$0.6M_{\odot}$ of radioactive ^{56}Ni, and the decay of this radioactive ^{56}Ni, not the explosion energy, powers the light curve. There is a correlation, obeyed by the vast majority of SNe Ia, between the peak brightness and the timescale over which the light curve decays from its maximum. This "brighter is broader" relation [3] explains the property of these events that allows their use as distance indicators—by observing the decline from maximum light, one can infer the peak brightness. The correlation is understood physically as stemming from having both the luminosity and opacity being set by the mass of 56Ni synthesized in the explosion [18,19,20].

1.1. Observational trends of SNe Ia

Many contemporary observations address correlations between the event and properties of the progenitor galaxy. Of particular interest are correlations between the brightness of an event and the isotopic composition of a galaxy and its age, measured by the intensity of star formation.

The proportion of material that has previously been processed in stars, i.e., elements other than hydrogen and helium, which are collectively referred to as "metals," is a measurable property of the galaxy. (The relative abundance of these elements is referred to as the galaxy's "metallicity.") The presence of these elements in a progenitor white dwarf influences the outcome of the explosion by changing the path of nuclear burning, which influences the amount of ^{56}Ni synthesized in an event. Because the decay of ^{56}Ni powers the light curve, metallicity can directly influence the brightness of an event. Observational results to date are consistent with a shallow dependence of brightness on metallicity, with dimmer events in metal-rich galaxies, but are unable demonstrate a conclusive trend [21,22,23,24]. Determining the metallicity dependence is challenging because the effect appears to be small, is difficult to measure, and there are systematic effects associated with the mass-metallicity relationship within galaxies [22]. This effect is also difficult to decouple from the apparently stronger effect of the age of the parent stellar population on the mean brightness of SNe Ia [22,24,25].

When galaxies form, they are rich in hydrogen gas and undergo a period of intense star formation. Observations also target correlations between the brightness of an event and the age of a galaxy measured as the elapsed time from the period of intense star formation. Some observations indicate that the dependence of the SN Ia rate on delay time (elapsed time between star formation and the supernova event) is best fit by a bimodal distribution with a prompt component less than 1 Gyr after star formation and a tardy component several Gyr later [26,27]. Other studies only indicate a correlation between the delay time and brightness of SNe Ia with dimmer events occurring at longer delay times [28,24,23,29].

1.2. The deflagration to detonation transition model

We explore the systematics of these events with models that assume the explosion occurs in a carbon-oxygen white dwarf that has gained mass from a companion. Here we briefly describe this explosion scenario and the physics involved.

The core of a white dwarf is dense enough that electrons are subject to quantum mechanical effects, specifically the Pauli exclusion principle, that prevents the electrons from occupying the same quantum states [30]. The result is that electrons are forced into higher energy states, and the reaction to this forcing acts as a pressure that supports the star. Matter in this high-density condition is said to be "degenerate," and the case of interest, a white dwarf that has gained mass from a companion, is known as the "single degenerate" scenario.

If a white dwarf gains mass from a binary companion, the central density and temperature increase, and the star may eventually collapse to a neutron star. For a white dwarf composed principally of carbon and oxygen, before the collapse can occur the density and temperature reach values at which carbon fusion begins and the star enters a period of simmering that drives convection in the core producing a growing convective zone [31,32]. After $\approx 10^3$ yr the local temperature is hot enough that the burning timescale becomes shorter than a convective turnover time so that a local patch runs away and a subsonic flame is born, initiating the explosion [32].

Early one-dimensional simulations of the single-degenerate case showed that the most successful scenario follows the initial deflagration (subsonic reaction front) with a (supersonic) detonation, i.e. a deflagration-detonation transition (DDT [33,34]). Models with such a delayed detonation naturally account for some spectral features and the chemical stratification observed in the ejecta [35]. While one-dimensional models are able to reproduce observed features of the light curve and spectra, much of the physics is missing. Of particular concern is the degree to which the white dwarf expands during the deflagration phase of the explosion, which multidimensional simulations show depends on the behavior of fluid instabilities at the flame front. The degree of expansion during the deflagration phase is critical to the explosion because it determines the density at which the majority of the stellar material burns, which in turn controls the nucleosynthetic yield. Capturing the effects of fluid instabilities is therefore essential to modeling this process and necessitates the development of multidimensional models. By relaxing the symmetry constraints on the model, buoyancy instabilities are naturally captured leading to a strong dependence on the initial conditions of the deflagration. Some cases with a DDT criterion based on previous one-dimensional studies indicated the result is too little expansion of the star prior to the detonation [36,37,38,39]. Multidimensional models, however, may reach the expected amount of expansion prior to the DDT with the choice of particular ignition conditions and thus retain the desirable features from one-dimensional models [40,41,42,43]. Our investigation centers on how properties of the progenitor white dwarf that follow from properties of the host galaxy or its evolutionary history influence this DDT scenario and hence the brightness of an event measured by the ^{56}Ni yield.

2. The Systematics of SNe Ia in the DDT Scenario

In Townsley et al. (2009) [44] we investigated the direct effect of reprocessed stellar material (metals) in the host galaxy via the initial neutron excess of the progenitor white dwarf. Because of weak interactions, metals produced by nuclear burning are more neutron rich than hydrogen and helium, and, accordingly, the neutron excess of these elements is thought to drive the explosion yield toward stable iron-group elements. Thus, there is relatively less radioactive ^{56}Ni in the NSE mix, which results in a dimmer event [45]. We investigated this effect by introducing ^{22}Ne into the progenitor white dwarf as a proxy for (neutron-rich) metals. The presence of ^{22}Ne influences the progenitor structure, the energy release of the burn, and the flame speed. The study was designed to measure how the ^{22}Ne content influences the competition between rising plumes and the expansion of the star, which determines the yield. We performed a suite of 20 DDT simulations varying only the initial ^{22}Ne in a progenitor model, and found a negligible effect on the pre-detonation expansion of the star and thus the yield of NSE material. The neutron excess sets the amount of material in NSE that favors stable

iron-group elements over radioactive ^{56}Ni. Our results were consistent with earlier work calculating the direct modification of ^{56}Ni mass from initial neutron excess [45].

In Jackson et al. (2010) [46] we expanded the Townsley et al. study to include the indirect effect of metallicity in the form of the ^{22}Ne mass fraction through its influence on the density at which the DDT takes place. We simulated 30 realizations each at 5 transition densities between $1 - 3 \times 10^7$ g cm^{-3} for a total of 150 simulations. We found a quadratic dependence of the NSE yield on the log of the transition density, which is determined by the competition between rising unstable plumes and stellar expansion. By then considering the effect of metallicity on the transition density, we found the NSE yield decreases slightly with metallicity, but that the ratio of the 56Ni yield to the overall NSE yield does not change as significantly. Observations testing the dependence of the yield on metallicity remain somewhat ambiguous, but the dependence we found is comparable to that inferred from [47]. We also found that the scatter in the results increases with decreasing transition density, and we attribute this increase in scatter to the nonlinear behavior of the unstable rising plumes.

In Krueger et al. (2010) [48] we investigated the effect of central density on the explosion yield. We found that the overall production of NSE material did not change, but there was a definite trend of decreasing ^{56}Ni production with increasing progenitor central density. We attribute this result to higher rates of weak interactions (electron captures) that produce a higher proportion of neutronized material at higher density. More neutronization means less symmetric nuclei like ^{56}Ni, and, accordingly, a dimmer event. This result may explain the observed decrease in SNe Ia brightness with increasing delay time. The central density of the progenitor is determined by its evolution, including the transfer of mass from the companion. If there is a long period of cooling before the onset of mass transfer, the central density of the progenitor will be higher when the core reaches the carbon ignition temperature, thereby producing less ^{56}Ni and thus a dimmer event. In addition, we found considerable variation in the trends from some realizations, stressing the importance of statistical studies.

Our approach in these investigations has been to isolate facets of the problem expected to follow from properties of the host galaxy or evolution history of the progenitor white dwarf and perform a controlled statistical analysis of a ensemble of multidimensional simulations (described below). Not surprisingly, many other possible systematic effects exist (outlined in [44]) that were held fixed in each study. The ultimate goal of our research into thermonuclear supernovae is to consider the interdependence of all of these effects in the construction of the full theoretical picture.

3. Methodology

Our methodology for the theoretical study of thermonuclear supernovae consists of four principal parts. First is the ability to construct parameterized, hydrostatic initial white dwarf progenitors that can freely change thermal and compositional structure to match features from the literature about progenitor models [46]. Second is a model flame and energetics scheme with which to track both (subsonic) deflagrations and (supersonic) detonations as well as the evolution of dynamic ash in NSE. This flame/energetics scheme is implemented in the Flash hydrodynamics code [49,50,51]. Third is utilization of a scheme to post-process the density and temperature histories of Lagrangian tracer particles with a detailed nuclear network in order to calculate detailed nucleosynthetic yields [52,53]. Fourth, we developed a statistical framework with which to perform ensembles of simulations for well-controlled studies of systematic effects. Below we highlight the flame model and the statistical framework. Complete details of the methodology can be found in previously published results [52,54,55,44,53].

3.1. Flame Model

The great disparity between the length scale of a white dwarf (~10^9 cm) and the width of laminar nuclear flame (<1 cm) necessitates the use of a model flame in simulations of thermonuclear supernovae. Even simulations with adaptive mesh refinement cannot resolve the actual diffusive flame front in a simulation of the event. The model we use propagates an artificially broadened flame front with an advection-diffusion-reaction (ADR) scheme [56,57] that has been demonstrated to be

acoustically quiet and produce a unique flame speed [55]. This scheme evolves a reaction progress variable ϕ, where $\phi = 0$ indicates unburned fuel and $\phi = 1$ indicates burned ash, with the advection-reaction-diffusion equation

$$\partial_t \phi + \vec{u} \cdot \nabla \phi = \kappa \nabla^2 \phi + \frac{1}{\tau} R(\phi) . \tag{1}$$

Here κ is a constant and $R(\phi)$ a non-dimensional function, and both are tuned to propagate the reaction front at the physical speed of the real flame [58,59] and to be just wide enough to be resolved in our simulation. We use a modified version of the KPP reaction rate discussed by [57], in which $R \propto (\phi - \varepsilon)(1 - \phi + \varepsilon)$, where $\simeq 10^{-3}$.

In simulating the deflagration phase, the flame front separates expanded burned material (the hot ash) from denser unburned stellar material (cold fuel). The expansion and buoyancy of the burned material forces the interface upward into the denser fuel, and the configuration is susceptible to the Rayleigh-Taylor fluid instability [60,61]. It is necessary to enhance the flame speed in order to prevent turbulence generated by the Raleigh-Taylor instability from destroying the artificially broadened flame front. In the simulations discussed here, the enhancement is accomplished by the method suggested by Khokhlov [56] in which we prevent the flame front speed, s, from falling below a threshold that is scaled with the strength of the Raleigh-Taylor instability on the scale of the flame front ($s \propto \sqrt{g\ell}$, where g is the local gravity and and ℓ is the width of the artificial flame, which is a few times the grid resolution). This scaling of the flame speed prevents the Rayleigh-Taylor instability from effectively pulling the flame apart and also mimics what is a real enhancement of the burning area that is occurring due to structure in the flame surface on unresolved scales. It is expected that, for much of the white dwarf deflagration, the flame is "self-regulated," in which the small scale structure of the flame surface is always sufficient to keep up with the large-scale buoyancy-driven motions of the burned material. Thus the actual burning rate is determined by this action, which is resolved in our simulations.

As seen in Figure 1, [55] and by [62], these techniques demonstrate a suitable level of convergence for studies such as ours. This technique does makes it necessary to explicitly drop s to zero below a density of 10^7 g cm^{-3}, approximately where the real flame will be extinguished. This prescription captures some effects of the Rayleigh-Taylor instability and maintains the integrity of the thickened flame, but it does not completely describe the flame-turbulence interaction. Also, we neglect any enhancement from background turbulence from convection prior to the birth of the flame. Future work will include physically-motivated models for these effects [63].

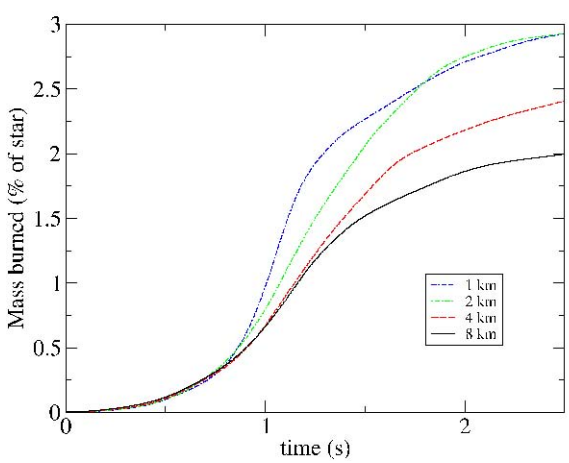

Figure 1. Fraction of star burned during the deflagration phase of a thermonuclear supernova for four two-dimensional simulations at varying resolutions. The initial conditions consisted of a 16 km ignition point started at a radius of 40 km from the center of the star. The result of this off-set ignition point is a single rising plume that may subsequently trigger a detonation [41]. Shown are effective resolutions of 8, 4, 2, and 1 km, and the results demonstrate reasonable convergence, especially during the early phases. Adapted from Townsley et al. (2009).

The model also includes the nuclear energy release occurring at the flame front and in the dynamic ash in NSE. We performed a detailed study of the nuclear processes occurring in a flame in the interior

of a white dwarf and developed an efficient and accurate method for incorporating the results into numerical simulations [54]. Tracking even tens of nuclear species is computationally prohibitive, and many more than this are required to accurately calculate the physics such as electron captures rates that are essential to studying rates of neutronization. We instead reproduce the energy release of the nuclear reactions with a highly abstracted model based on tabulation of properties of the burned material calculated in our study of the relevant nuclear processes.

The nuclear processing can be well approximated as a three stage process: initially carbon is consumed, followed by oxygen, which creates a mixture of silicon-group and light elements that is in nuclear statistical quasi-equilibrium (NSQE), finally the silicon-group nuclei are converted to iron-group, reaching full NSE. In both of these equilibrium states, the capture and creation of light elements (via photodisintegration) is balanced, so that energy release can continue by changing the relative abundance of light (low nuclear binding energy) and heavy (high nuclear binding energy) nuclides, an action that releases energy as buoyant burned material rises and expands. We track each of these stages with separate progress variables and separate relaxation times derived from full nuclear network calculations [54]. We define three progress variables representing consumption of carbon ϕ_C, consumption of oxygen to material in NSQE, ϕ_{NSQE}, and conversion of silicon to iron group nuclides to form true NSE material, ϕ_{NSE}. The physical state of the fluid is tracked with the electron number per baryon, Y_e, the number of nuclei per baryon, Y_i, and the average binding energy per baryon, $\bar{q}$, the minimum properties necessary to hydrodynamically evolve the fluid. Carbon consumption is coupled directly to the flame progress variable, $\phi_C \equiv \phi$, from eq. (1) above, and the later flame stages follow using simple relationships from more detailed calculations.

Burning and evolution of post-flame material change the nuclear binding energy, and we use the binding energy of magnesium to approximate the intermediate burning products of carbon. The method is finite differenced in such a way to ensure explicit conservation of energy. Weak processes (e.g., electron capture) are included in the calculation of the energy input rate, as are neutrino losses, which are calculated by convolving the NSE distribution with the weak interaction cross sections. Tracking the conversion of silicon-group nuclides to the iron-group is important for studying the effects of electron capture because the thresholds are lower for the iron-group nuclides. Both the NSE state and the electron capture rates were calculated with a set of 443 nuclides including all which have weak interaction cross sections given by [64]. This treatment of electron capture in the energy release is the most realistic currently in use for thermonuclear supernovae. Electron capture feeds back on the hydrodynamics in three ways: the NSE can shift to more tightly bound elements as the electron fraction, Y_e, changes, releasing some energy and changing the local temperature; also the reduction in Y_e lowers the Fermi energy, reducing the primary pressure support of this highly degenerate material and having an impact on the buoyancy of the neutronized material; finally neutrinos are emitted (since the star is transparent to them) so that some energy is lost from the system.

In addition to all of these effects during the deflagration phase of SNe Ia, the progress-variable-based method has been extended to model the gross features of detonations [65,53]. Instead of coupling the first burning stage, ϕ_C, representing carbon consumption, to the ADR flame front, we instead can use the actual temperature-dependent rate for carbon burning, or possibly a more appropriate effective rate. Doing so allows shock propagation to trigger burning and therefore create a propagating detonation. This method has been used successfully by [66] in modern studies of the DDT, and our multistage burning model shares many features with theirs (see also [67] and [68]). We treat the later burning stages very similarly, though we have taken slightly more care to track the intermediate stages and have nearly eliminated acoustic noise when coupling energy release to the flame.

Results from a two-dimensional DDT simulation utilizing these capabilities are shown in Figure 2. The three panels illustrate the early deflagration phase, the configuration just prior to ignition of the first detonation, and the progress of the detonation. The blue contour marks the division between the pre-explosion convective core, which has C/O/^{22}Ne composition of 30/66/4% by mass, and an outer

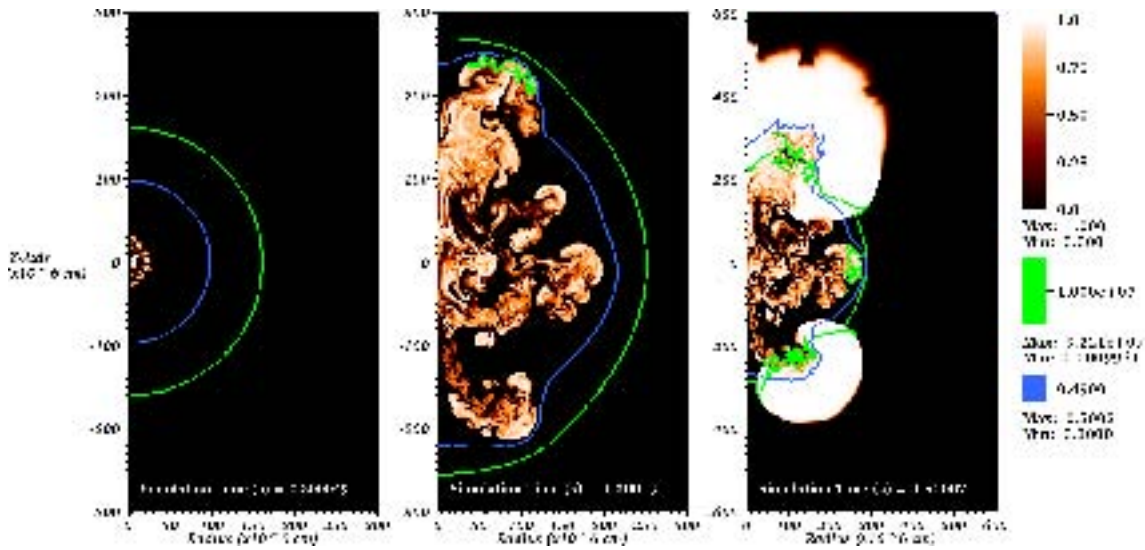

Figure 2. Images from a two-dimensional SNe Ia simulation from a neutronized-core progenitor. The left panel shows the development of fluid instabilities during the early deflagration phase, the center panel shows the configuration just prior to the first detonation, and the right panel shows the configuration with two distinct detonations consuming the star. Shown in color scale is the carbon-burning reaction progress variable which evolves from 0 to 1 and contours of $\rho = 10^7$ g cm^{-3} (green) and where the initial $X_{^{12}C} = 0.49$ (blue). The latter, initially inner, contour indicates the separation between the convective, low C-abundance, neutronized core and the higher C surface layers. Note that the scale on the right panel is twice that of the first two in order to accommodate the expansion of the star.

region with a composition of 50/48/2%. The contrast in C/O abundance reflects the stellar evolution of the progenitor, during which the central regions are produced by convective core helium burning, while the outer layers are produced by shell burning during the asymptotic giant branch phase [69]. The contrast in ^{22}Ne is due to production during the simmering phase.

3.2. Statistical Framework

We also developed a theoretical framework for the study of systematic effects in SNe Ia that will utilize two-and three-dimensional simulations in the DDT paradigm [44]. This framework allows the evaluation of the average dependence of the properties of SNe Ia on underlying parameters, such as composition, by constructing a theoretical sample based on a probabilistic initial ignition condition. Such sample-averaged dependencies are important for understanding how SN Ia models may explain features of the observed sample, particularly samples generated by large dark energy surveys utilizing SNe Ia as distance indicators.

The theoretical sample is constructed to represent statistical properties of the observed sample of SNe Ia such as the mean inferred ^{56}Ni yield and variance. Within the DDT paradigm, the variance in ^{56}Ni yields can be explained by the development of fluid instabilities during the deflagration phase of the explosion. By choice of the initial configuration of the flame, we may influence the growth of these fluid instabilities resulting in varying amounts of ^{56}Ni synthesized during the explosion. [44] found that perturbing a spherical flame surface with radius (r_0 = 150 km) with spherical harmonic modes (Y_l^m) between $12 \leq l \leq 16$ with random amplitudes (A) normally distributed between 0–15 km and, for 3D, random phases (δ) uniformly distributed between $-\pi - \pi$ best characterized the mean inferred ^{56}Ni yield and sample variance from observations:

$$r(\theta) = r_0 + \sum_{l=l_{\min}}^{l_{\max}} A_l Y_l(\theta) \quad (2)$$

$$r(\theta,\phi) = r_0 + \sum_{l=l_{\min}}^{l_{\max}} \sum_{m=-l}^{l} \frac{A_l^m e^{i\delta_l^m}}{\sqrt{2l+1}} Y_l^m(\theta,\phi). \quad (3)$$

With a suitable random-number generator, a sample population of progenitor WDs is constructed by defining the initial flame surface for a particular progenitor.

4. Statistical properties of the simulations

For this contribution, we focus on the ensemble of simulations from the central density study. In this study, the measure of the explosion is the yield of radioactive ^{56}Ni, the decay of which powers the light curve. In comparing a simulated explosion to astronomical observations, the results from simulations must be considered at frequencies of light corresponding to the bands in which the observations are made. We applied a simple relationship between the mass of ^{56}Ni synthesized in the explosion and the peak brightness in the V band. Thus the assumption for these models that the amount of ^{56}Ni synthesized in the explosion directly corresponds to the peak V-band brightness [24,70,71].

In the study, we found considerable variation in the amount of synthesized ^{56}Ni that we attribute to differences in the evolution during the deflagration phase of the explosion. As described above, the initial conditions for a realization were established stochastically. The deeply non-linear behavior of the subsequent evolution the buoyant rising plumes results in considerable variation in the duration of the deflagration phase, which is set by the time required for the first plume to rise to the DDT density. During the deflagration, the star reacts to the subsonic burning and expands. When a plume reaches the DDT threshold, the subsequent detonation very rapidly incinerates the expanded star (see Figure 2 for an illustration). ^{56}Ni is synthesized when stellar material burns at relatively high densities, so the amount of expansion determines the mass of material that will burn to ^{56}Ni. Thus the evolution during the deflagration, particularly its duration, strongly influences the ^{56}Ni yield. From this "noisy" background we were able to find a trend of decreased ^{56}Ni yield with increasing central density.

Figure 3 plots the mass of ^{56}Ni as a function of central density, illustrating the trend and scatter in our ensemble of simulations. Shown are the average among realizations, the standard deviation, and the standard error. Note that the standard deviation of our sample is about as large as the limits of the trend. Realizations 2, 4, and 8 in the figure exemplify the variation with progenitor central density, specifically the non-monotonicity of the individual trends. While these three realizations show a decreasing standard deviation with increasing central density, when considering the entire sample population, the standard deviation remains approximately the same as a function of central density. Table 1 provides the minima, mean, maxima, and standard deviations for ^{56}Ni and NSE masses at each central density.

In order to obtain a statistically meaningful trend, we must first demonstrate that our sample size characterizes the properties of the population. In Figure 4, we show that the standard deviation of the ^{56}Ni mass converges for all progenitor central densities with 15–20 realizations. Second, we must perform a number of realizations (take enough samples) such that the standard error of the mean is small enough to produce a statistically meaningful average trend. In the case that no trend exists, the number or realizations provides a limit to the magnitude of the mean trend. The standard error of the mean is computed to be the standard deviation divided by the square root of the number of samples.

We analyzed the trend of ^{56}Ni mass with progenitor central density with 30 realizations. While not shown graphically, the NSE mass does not vary significantly with central density. We evaluate an upper limit to the trend to be a decrease of 0.006 solar masses of NSE per 10^9 g cm^{-3} of central density. That result translates to less than a 0.6% change in the NSE yield per 10^9 g cm^{-3}. From Figures 3 and 4, we conclude that a statistical approach is necessary to evaluate systematic trends in highly nonlinear problems, such as SNe Ia.

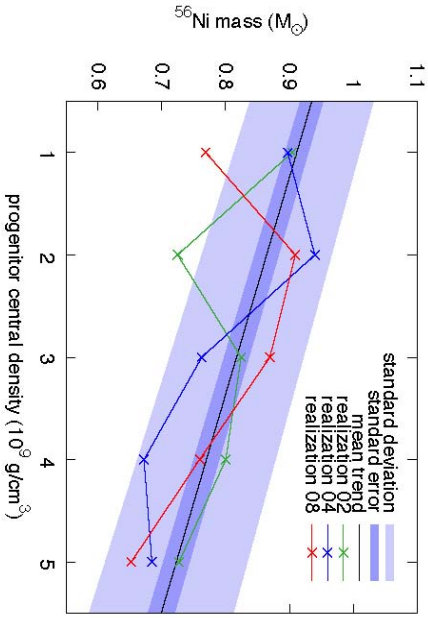

Figure 3. Relationship between mass of ^{56}Ni produced in a simulated event and central density of the progenitor white dwarf when the deflagration is ignited. The light purple is the standard deviation, the dark purple is the standard error of the mean, and the black line is the mean trend. Also shown are the trends for three different initial configurations as the central density varies. These three configurations do not match the statistical trend, nor are they monotonic; from this we conclude that a statistical study is important when considering a highly nonlinear problem such as a SN Ia. Adapted from Krueger et al. (2010) [48].

Table 1. Minima, means (μ), maxima, and standard deviations (σ) of ^{56}Ni and NSE masses from central density study. All masses are in units of M8.

ρ_c (g/cm^3)		1.000E+9	2.000E+9	3.000E+9	4.000E+9	5.000E+9
^{56}Ni	min	6.920E–1	6.905E–1	5.657E–1	5.828E–1	5.304E–1
	μ	9.105E–1	8.723E–1	8.035E–1	7.713E–1	7.255E–1
	max	1.052E+0	1.034E+0	9.813E–1	9.640E–1	9.288E–1
	σ	9.638E–2	9.945E–2	1.109E–1	1.091E–1	1.078E–1
NSE	min	7.969E–1	8.565E–1	7.783E–1	8.450E–1	8.197E–1
	μ	1.032E+0	1.050E+0	1.028E+0	1.038E+0	1.026E+0
	max	1.187E+0	1.225E+0	1.216E+0	1.228E+0	1.231E+0
	σ	1.039E–1	1.044E–1	1.149E–1	1.101E–1	1.082E–1

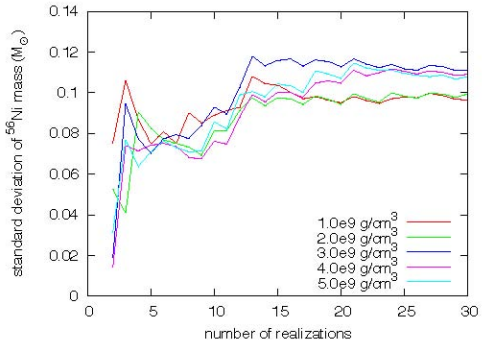

Figure 4. Convergence of the standard deviation of the mass as the data ^{56}Ni sample size increases for each of the five progenitor central densities. Each "realization" constitutes a unique initial condition configuration. Around 15–20 realizations achieve approximately the final standard deviation. The convergence of the standard deviation suggests that a sufficient number of data points have been included to compute a statistically correct mean.

5. Conclusions

Many studies have shown that small changes to the chosen initial conditions of a SNe Ia model result in large changes to the outcome of the explosion due to the non-linear effect of fluid instabilities. Our statistical framework relies on this property of multi-dimensional SNe Ia simulations to produce a sample population representative of the observed population. However, for the first time, we have

demonstrated that these small changes to the initial conditions can also influence systematic trends with properties of the progenitor WD such as central density. The effect of varying central density within a single realization does not characterize the entire sample population! In fact, each realization's outcome varies in a different way with changing central density as shown in Figure 3. It is only when all realizations in the sample population are considered that a meaningful and statistically significant trend emerges.

By varying the central density in a progenitor WD model, we also vary the density structure. The speed of the laminar flame depends on the density of the fuel it consumes. In hindsight, it is not that surprising that varying the fuel density of the initial flame results in non-linear behavior of the resulting supernovae similar to the effect of varying the initial position of the flame surface. Therefore, we must use a statistical ensemble of simulations to evaluate systematic trends in multi-dimensional SNe Ia that are subject to fluid instabilities.

In future studies we plan to explore systematic effects due to varying the core carbon-tooxygen (C/O) ratio. The core C/O ratio is thought to vary with zero-age main sequence mass of the progenitor WD, metallicity, and the mass of the companion star [72]. Because the laminar flame speed also depends on the carbon abundance in the fuel, a statistical ensemble of simulations will be necessary to evaluate this effect. It is not clear whether the results of [42] are characteristic of the observed sample of SNe Ia because a statistical approach was not employed.

Acknowledgments

This work was supported by the Department of Energy through grants DE-FG02-07ER41516, DE-FG02-08ER41570, and DE-FG02-08ER41565, and by NASA through grant NNX09AD19G. ACC also acknowledges support from the Department of Energy under grant DE-FG0287ER40317. DMT received support from the Bart J. Bok fellowship at the University of Arizona for part of this work. The authors acknowledge the hospitality of the Kavli Institute for Theoretical Physics, which is supported by the NSF under grant PHY05-51164, during the programs "Accretion and Explosion: the Astrophysics of Degenerate Stars" and "Stellar Death and Supernovae." The software used in this work was in part developed by the DOE-supported ASC/Alliances Center for Astrophysical Thermonuclear Flashes at the University of Chicago. This work was also supported in part by the US Department of Energy, Office of Nuclear Physics, under contract DE-AC02-06CH11357 and utilized resources at the New York Center for Computational Sciences at Stony Brook University/Brookhaven National Laboratory which is supported by the U.S. Department of Energy under Contract No. DE-AC02-98CH10886 and by the State of New York.

References

[1] A. V. Filippenko. Optical spectra of supernovae. *Annu. Rev. Astron. Astrophys*, 35:309–355, 1997.

[2] W. Hillebrandt and J. C. Niemeyer. Type Ia supernova explosion models. *Annu. Rev. Astron. Astrophys*, 38:191, 2000.

[3] M. M. Phillips. The absolute magnitudes of type Ia supernovae. *Astrophysical Journal Letters*, 413:L105, 1993.

[4] A. G. Riess, W. H. Press, and R. P. Kirshner. A Precise Distance Indicator: Type IA Supernova Multicolor Light-Curve Shapes. *Astrophysical Journal*, 473:88–+, December 1996.

[5] A. Albrecht, G. Bernstein, R. Cahn, W. L. Freedman, J. Hewitt, W. Hu, J. Huth, M. Kamionkowski, E. W. Kolb, L. Knox, J. C. Mather, S. Staggs, and N. B. Suntzeff. Report of the Dark Energy Task Force. *ArXiv Astrophysics e-prints*, astro-ph/0609591, September 2006.

[6] A. G. Riess, A. V. Filippenko, P. Challis, A. Clocchiatti, A. Diercks, P. M. Garnavich, R. L. Gilliland, C. J. Hogan, S. Jha, R. P. Kirshner, B. Leibundgut, M. M. Phillips, D. Reiss, B. P. Schmidt, R. A. Schommer, R. C. Smith, J. Spyromilio, C. Stubbs, N. B. Suntzeff, and J. Tonry. Observational evidence from supernovae for an accelerating universe and a cosmological constant. *Astronomical Journal*, 116:1009, 1998.

[7] S. Perlmutter, G. Aldering, G. Goldhaber, R. A. Knop, P. Nugent, P. G. Castro, S. Deustua, S. Fabbro, A. Goobar, D. E. Groom, I. M. Hook, A. G. Kim, M. Y. Kim, J. C. Lee, N. J. Nunes, R. Pain, C. R. Pennypacker, R. Quimby, C. Lidman, R. S. Ellis, M. Irwin, R. G. McMahon, P. Ruiz-Lapuente, N. Walton, B. Schaefer, B. J. Boyle, A. V. Filippenko, T. Matheson, A. S. Fruchter, N. Panagia, H. J. M. Newberg, W. J. Couch, and The Supernova Cosmology Project. Measurements of Omega and Lambda from 42 high-redshift supernovae. *Astrophysical Journal*, 517:565, 1999.

[8] E. Kolb et al. Report of the Dark Energy Task Force. electronic, June 2006. http://www.science.doe.gov/hep/DETF-FinalRptJune30,2006.pdf.

[9] M. Hicken, W. M. Wood-Vasey, S. Blondin, P. Challis, S. Jha, P. L. Kelly, A. Rest, and R. P. Kirshner. Improved Dark Energy Constraints from ˜100 New CfA Supernova Type Ia Light Curves. *Astrophysical Journal*, 700:1097–1140, August 2009.

[10] H. Lampeitl, R. C. Nichol, H.-J. Seo, T. Giannantonio, C. Shapiro, B. Bassett, W. J. Percival, T. M. Davis, B. Dilday, J. Frieman, P. Garnavich, M. Sako, M. Smith, J. Sollerman, A. C. Becker, D. Cinabro, A. V. Filippenko, R. J. Foley, C. J. Hogan, J. A. Holtzman, S. W. Jha, K. Konishi, J. Marriner, M. W. Richmond, A. G. Riess, D. P. Schneider, M. Stritzinger, K. J. van der Heyden, J. T. Vanderplas, J. C. Wheeler, and C. Zheng. First-year Sloan Digital Sky Survey-II supernova results: consistency and constraints with other intermediate-redshift data sets. *Monthly Notices of the Royal Astronomical Society*, 401:2331–2342, February 2010.

[11] R. P. Kirshner. Foundations of Supernova Cosmology. *ArXiv e-prints*, October 2009.

[12] J. W. Truran and A. G. W. Cameron. Evolutionary Models of Nucleosynthesis in the Galaxy. *Ap&SS*, 14:179–222, November 1971.

[13] D. A. Howell, A. Conley, M. Della Valle, P. E. Nugent, S. Perlmutter, G. H. Marion, K. Krisciunas, C. Badenes, P. Mazzali, G. Aldering, P. Antilogus, E. Baron, A. Becker, C. Baltay, S. Benetti, S. Blondin, D. Branch, E. F. Brown, S. Deustua, A. Ealet, R. S. Ellis, D. Fouchez, W. Freedman, A. Gal-Yam, S. Jha, D. Kasen, R. Kessler, A. G. Kim, D. C. Leonard, W. Li, M. Livio, D. Maoz, F. Mannucci, T. Matheson, J. D. Neill, K. Nomoto, N. Panagia, K. Perrett, M. Phillips, D. Poznanski, R. Quimby, A. Rest, A. Riess, M. Sako, A. M. Soderberg, L. Strolger, R. Thomas, M. Turatto, S. van Dyk, and W. M. Wood-Vasey. Type Ia supernova science 2010–2020. *ArXiv e-prints*, March 2009. 0903.1086.

[14] N. Gehrels. Report on the science coordination group activities for the joint dark energy mission (jdem). Technical report, Goddard Space Flight Center, 2009.

[15] R. A. Scalzo, G. Aldering, P. Antilogus, C. Aragon, S. Bailey, C. Baltay, S. Bongard, C. Buton, M. Childress, N. Chotard, Y. Copin, H. K. Fakhouri, A. Gal-Yam, E. Gangler, S. Hoyer, M. Kasliwal, S. Loken, P. Nugent, R. Pain, E. Pécontal, R. Pereira, S. Perlmutter, D. Rabinowitz, A. Rau, G. Rigaudier, K. Runge, G. Smadja, C. Tao, R. C. Thomas, B. Weaver, and C. Wu. Nearby Supernova Factory Observations of SN 2007if: First Total Mass Measurement of a Super-Chandrasekhar-Mass Progenitor. *Astrophysical Journal*, 713:1073–1094, April 2010.

[16] F. Yuan, R. M. Quimby, J. C. Wheeler, J. Vinkó, E. Chatzopoulos, C. W. Akerlof, S. Kulkarni, J. M. Miller, T. A. McKay, and F. Aharonian. The Exceptionally Luminous Type Ia Supernova 2007if. *Astrophysical Journal*, 715:1338–1343, June 2010.

[17] M. Gilfanov and Á. Bogdán. An upper limit on the contribution of accreting white dwarfs to the typeIa supernova rate. *Nature*, 463:924–925, February 2010.

[18] W. D. Arnett. Type I supernovae. I—analytic solutions for the early part of the light curve. *Astrophysical Journal*, 253:785, 1982.

[19] P. A. Pinto and R. G. Eastman. The physics of type Ia supernova light curves. I. analytic results and time dependence. *Astrophysical Journal*, 530:744–756, 2000.

[20] D. Kasen and S. E. Woosley. On the Origin of the Type Ia Supernova Width-Luminosity Relation. *Astrophysical Journal*, 656:661–665, February 2007.

[21] J. S. Gallagher, P. M. Garnavich, P. Berlind, P. Challis, S. Jha, and R. P. Kirshner. Chemistry and Star Formation in the Host Galaxies of Type Ia Supernovae. *Astrophysical Journal*, 634:210–226, November 2005.

[22] J. S. Gallagher, P. M. Garnavich, N. Caldwell, R. P. Kirshner, S. W. Jha, W. Li, M. Ganeshalingam, and A. V. Filippenko. Supernovae in Early-Type Galaxies: Directly Connecting Age and Metallicity with Type Ia Luminosity. *Astrophysical Journal*, 685:752–766, October 2008.

[23] J. D. Neill, M. Sullivan, D. A. Howell, A. Conley, M. Seibert, D. C. Martin, T. A. Barlow, K. Foster, P. G. Friedman, P. Morrissey, S. G. Neff, D. Schiminovich, T. K. Wyder, L. Bianchi, J. Donas, T. M. Heckman, Y.-W. Lee, B. F. Madore, B. Milliard, R. M. Rich, and A. S. Szalay. The Local Hosts of Type Ia Supernovae. *Astrophysical Journal*, 707:1449–1465, December 2009.

[24] D. A. Howell, M. Sullivan, E. F. Brown, A. Conley, D. LeBorgne, E. Y. Hsiao, P. Astier, D. Balam, C. Balland, S. Basa, R. G. Carlberg, D. Fouchez, J. Guy, D. Hardin, I. M. Hook, R. Pain, K. Perrett, C. J. Pritchet, N. Regnault, S. Baumont, J. LeDu, C. Lidman, S. Perlmutter, N. Suzuki, E. S. Walker, and J. C. Wheeler. The Effect of Progenitor Age and Metallicity on Luminosity and ^{56}Ni Yield in Type Ia Supernovae. *Astrophysical Journal*, 691:661–671, January 2009.

[25] B. K. Krueger, A. P. Jackson, D. M. Townsley, A. C. Calder, E. F. Brown, and F. X. Timmes. On Variations of the Brightness of Type Ia Supernovae with the Age of the Host Stellar Population. *Astrophysical Journal Letters*, submitted, 2010.

[26] F. Mannucci, M. Della Valle, and N. Panagia. Two populations of progenitors for Type Ia supernovae? *Monthly Notices of the Royal Astronomical Society*, 370:773–783, August 2006.

[27] C. Raskin, E. Scannapieco, J. Rhoads, and M. Della Valle. Prompt Ia Supernovae are Significantly Delayed. *Astrophysical Journal*, 707:74–78, December 2009.

[28] J. S. Gallagher, P. M. Garnavich, N. Caldwell, R. P. Kirshner, S. W. Jha, W. Li, M. Ganeshalingam, and A. V. Filippenko. Supernovae in Early-Type Galaxies: Directly Connecting Age and Metallicity with Type Ia Luminosity. *Astrophysical Journal*, 685:752–766, October 2008.

[29] T. D. Brandt, R. Tojeiro, É. Aubourg, A. Heavens, R. Jimenez, and M. A. Strauss. The Ages of Type Ia Supernova Progenitors. *ArXiv e-prints*, February 2010.

[30] R. H. Dicke and J. P. Wittke. *Introduction to Quantum Mechanics*. Addison-Wesley, Reading, 1960.

[31] S. E. Woosley, S. Wunsch, and M. Kuhlen. Carbon Ignition in Type Ia Supernovae: An Analytic Model. *Astrophysical Journal*, 607:921–930, June 2004.

[32] M. Zingale, A. S. Almgren, J. B. Bell, A. Nonaka, and S. E. Woosley. Low Mach Number Modeling of Type IA Supernovae. IV. White Dwarf Convection. *Astrophysical Journal*, 704:196–210, October 2009.

[33] A. M. Khokhlov. Delayed detonation model for type IA supernovae. *Astronomy and Astrophysics*, 245:114–128, May 1991.

[34] P. Höflich and A. Khokhlov. Explosion Models for Type IA Supernovae: A Comparison with Observed Light Curves, Distances, H 0, and Q 0. *Astrophysical Journal*, 457:500–+, February 1996.

[35] D. Kasen and T. Plewa. Spectral Signatures of Gravitationally Confined Thermonuclear Supernova Explosions. *Astrophysical Journal Letters*, 622:L41–L44, March 2005.

[36] J. C. Niemeyer, W. Hillebrandt, and S. E. Woosley. Off-Center Deflagrations in Chandrasekhar Mass Type IA Supernova Models. *Astrophysical Journal*, 471:903–+, November 1996.

[37] A. C. Calder, T. Plewa, N. Vladimirova, E. F. Brown, D. Q. Lamb, K. Robinson, and J. W. Truran. Deflagrating white dwarfs: a Type Ia supernova model. In *Bulletin of the American Astronomical Society*, volume 35 of *Bulletin of the American Astronomical Society*, pages 1278–+, December 2003.

[38] A. C. Calder, T. Plewa, N. Vladimirova, D. Q. Lamb, and J. W. Truran. Type Ia Supernovae: An Asymmetric Deflagration Model. *ArXiv Astrophysics e-prints*, May 2004. astro-ph/0405162.
[39] E. Livne, S. M. Asida, and P. Höflich. On the Sensitivity of Deflagrations in a Chandrasekhar Mass White Dwarf to Initial Conditions. *Astrophysical Journal*, 632:443–449, October 2005.
[40] V. N. Gamezo, A. M. Khokhlov, and E. S. Oran. Deflagrations and detonations in thermonuclear supernovae. *Physical Review Letters*, 92:211102, 2004.
[41] T. Plewa, A. C. Calder, and D. Q. Lamb. Type Ia supernova explosion: Gravitationally confined detonation. *Astrophysical Journal Letters*, 612:L37–L40, 2004.
[42] F. K. Röpke, M. Gieseler, M. Reinecke, C. Travaglio, and W. Hillebrandt. Type Ia Supernova Diversity in Three-Dimensional Models. *Astronomy and Astrophysics*, 453:203, 2006.
[43] G. C. Jordan, IV, R. T. Fisher, D. M. Townsley, A. C. Calder, C. Graziani, S. Asida, D. Q. Lamb, and J. W. Truran. Three-Dimensional Simulations of the Deflagration Phase of the Gravitationally Confined Detonation Model of Type Ia Supernovae. *Astrophysical Journal*, 681:1448–1457, July 2008.
[44] D. M. Townsley, A. P. Jackson, A. C. Calder, D. A. Chamulak, E. F. Brown, and F. X. Timmes. Evaluating Systematic Dependencies of Type Ia Supernovae: The Influence of Progenitor ^{22}Ne Content on Dynamics. *Astrophysical Journal*, 701:1582–1604, August 2009.
[45] F. X. Timmes, E. F. Brown, and J. W. Truran. On variations in the peak luminosity of type Ia supernovae. *Astrophysical Journal*, 590:L83, 2003.
[46] A. P. Jackson, A. C. Calder, D. M. Townsley, D. A. Chamulak, E. F. Brown, and F. X. Timmes. On variations of the brightness of type Ia supernovae with the age of the host stellar population. *Astrophysical Journal*, 2010. submitted.
[47] E. Bravo, I. Domínguez, C. Badenes, L. Piersanti, and O. Straniero. Metallicity as a Source of Dispersion in the SNIa Bolometric Light Curve Luminosity-Width Relationship. *Astrophysical Journal Letters*, 711:L66–L70, March 2010.
[48] B. K. Krueger, A. P. Jackson, D. M. Townsley, A. C. Calder, E. F. Brown, and F. X. Timmes. Evaluating Systematic Dependencies of Type Ia Supernovae: The Influence of Deflagration to Detonation Density. *Astrophysical Journal*, 2010. submitted.
[49] B. Fryxell, K. Olson, P. Ricker, F. X. Timmes, M. Zingale, D. Q. Lamb, P. MacNeice, R. Rosner, J. W. Truran, and H. Tufo. FLASH: An adaptive mesh hydrodynamics code for modeling astrophysical thermonuclear flashes. *Astrophysical Journal Supplement*, 131:273–334, 2000.
[50] A. C. Calder, B. C. Curtis, L. J. Dursi, B. Fryxell, G. Henry, P. MacNeice, K. Olson, P. Ricker, R. Rosner, F. X. Timmes, H. M. Tufo, J. W. Truran, and M. Zingale. High-performance reactive fluid flow simulations using adaptive mesh refinement on thousands of processors. In *Proceedings of Supercomputing 2000*, page http://sc2000.org, 2000.
[51] A. C. Calder, B. Fryxell, T. Plewa, R. Rosner, L. J. Dursi, V. G. Weirs, T. Dupont, H. F. Robey, J. O. Kane, B. A. Remington, R. P. Drake, G. Dimonte, M. Zingale, F. X. Timmes, K. Olson, P. Ricker, P. MacNeice, and H. M. Tufo. On validating an astrophysical simulation code. *Astrophysical Journal Supplement*, 143:201–229, 2002.
[52] E. F. Brown, A. C. Calder, T. Plewa, P. M. Ricker, K. Robinson, and J. B. Gallagher. Type Ia supernovae: Simulations and nucleosynthesis. *Nucl. Phys. A*, 758:451, 2005.
[53] D. M. Townsley, F. X. Timmes, A. P. Jackson, A. C. Calder, and Brown. Nucleosynthesis During a Deflagration Detonation Transition Supernova Type Ia. *Astrophysical Journal*, 2010. to be submitted.
[54] A. C. Calder, D. M. Townsley, I. R. Seitenzahl, F. Peng, O. E. B. Messer, N. Vladimirova, E. F. Brown, J. W. Truran, and D. Q. Lamb. Capturing the Fire: Flame Energetics and Neutronization for Type Ia Supernova Simulations. *Astrophysical Journal*, 656:313–332, February 2007.
[55] D. M. Townsley, A. C. Calder, S. M. Asida, I. R. Seitenzahl, F. Peng, N. Vladimirova, D. Q. Lamb, and J. W. Truran. Flame Evolution During Type Ia Supernovae and the Deflagration

Phase in the Gravitationally Confined Detonation Scenario. *Astrophysical Journal*, 668:1118–1131, October 2007.

[56] A. M. Khokhlov. Propagation of turbulent flames in supernovae. *Astrophysical Journal*, 449:695, 1995.

[57] N. Vladimirova, G. Weirs, and L. Ryzhik. Flame capturing with an advection-reaction-diffusion model. *Combust. Theory Modelling*, 10(5):727–747, 2006.

[58] F. X. Timmes and S. E. Woosley. The conductive propagation of nuclear flames. I—Degenerate C + O and O + Ne + Mg white dwarfs. *Astrophysical Journal*, 396:649, 1992.

[59] D. A. Chamulak, E. F. Brown, and F. X. Timmes. The Laminar Flame Speedup by ^{22}Ne Enrichment in White Dwarf Supernovae. *Astrophysical Journal Letters*, 655:L93, February 2007.

[60] G. Taylor. The Instability of Liquid Surfaces when Accelerated in a Direction Perpendicular to their Planes. I. *Royal Society of London Proceedings Series A*, 201:192–196, March 1950.

[61] S. Chandrasekhar. *Hydrodynamic and Hydromagnetic Stability*. Dover, New York, 1981.

[62] V. N. Gamezo, A. M. Khokhlov, E. S. Oran, A. Y. Chtchelkanova, and R. O. Rosenberg. Thermonuclear supernovae: Simulations of the deflagration stage and their implications. *Science*, 299:77, 2003.

[63] A. P. Jackson, D. M. Townsley, and A. C. Calder. in preparation, 2010.

[64] K. Langanke and G. Mart´ınez-Pinedo. Rate tables for the weak processes of pf-shell nuclei in stellar environments. *At. Data Nucl. Data Tables*, 79:1, 2001.

[65] C. A. Meakin, I. Seitenzahl, D. Townsley, G. C. Jordan, J. Truran, and D. Lamb. Study of the Detonation Phase in the Gravitationally Confined Detonation Model of Type Ia Supernovae. *Astrophysical Journal*, 693:1188–1208, March 2009.

[66] V. N. Gamezo, A. M. Khokhlov, and E. S. Oran. Three-dimensional delayed-detonation model of type Ia supernovae. *Astrophysical Journal*, 623:337–346, April 2005.

[67] A. M. Khokhlov. Delayed detonation model for type Ia supernovae. *Astronomy and Astrophysics*, 245:114–128, 1991.

[68] A. M. Khokhlov. Three-Dimensional Modeling of the Deflagration Stage of a Type Ia Supernova Explosion. *Astrophysical Journal*, submitted, astro-ph/0008463, 2000.

[69] O. Straniero, I. Dom´ınguez, G. Imbriani, and L. Piersanti. The Chemical Composition of White Dwarfs as a Test of Convective Efficiency during Core Helium Burning. *Astrophysical Journal*, 583:878–884, February 2003.

[70] G. Goldhaber, D. E. Groom, A. Kim, G. Aldering, P. Astier, A. Conley, S. E. Deustua, R. Ellis, S. Fabbro, A. S. Fruchter, A. Goobar, I. Hook, M. Irwin, M. Kim, R. A. Knop, C. Lidman, R. McMahon, P. E. Nugent, R. Pain, N. Panagia, C. R. Pennypacker, S. Perlmutter, P. Ruiz-Lapuente, B. Schaefer, N. A. Walton, and T. York. Timescale Stretch Parameterization of Type Ia Supernova B-Band Light Curves. *Astrophysical Journal*, 558:359–368, September 2001.

[71] M. M. Phillips, P. Lira, N. B. Suntzeff, R. A. Schommer, M. Hamuy, and J. Maza. The reddening-free decline rate versus luminosity relationship for type Ia supernovae. *Astronomical Journal*, 118:1766–1776, 1999.

[72] H. Umeda, K. Nomoto, H. Yamaoka, and S. Wanajo. Evolution of 3–9 $M_{\odot}$ stars for $Z = 0.001$–0.03 and metallicity effects on type Ia supernovae. *Astrophysical Journal*, 513:861–868, 1999.